INTERNATIONAL JOURNAL OF ADVANCE RESEARCH, IDEAS AND INNOVATIONS IN TECHNOLOGY

ISSN: 2454-132X
Impact factor: 4.295
(Volume3, Issue1)

Preparation, Structure, and Characterization of $Nd_2mo_2o_9$ fast Oxide Ion Conductor

M. Rajasekhar
Advanced Energy Research Lab,
PG& Research Department of chemistry,
Government Arts College, Dharmapuri-636 705, South India.
Energylag20@gmail.com

N. Kalaivani
Advanced Energy Research Lab,
PG& Research Department of chemistry,
Government Arts College, Dharmapuri-636 705, South India.
Energylag20@gmail.com

Abstract: ***The structure and ion conductivity of $Nd_2Mo_2O_9$powders were synthesized by using $Nd(NO_2)_3$, MoO_3, and aspartic acid (fuel) in assisted combustion method with heating at 550˚C for 6 hours. The thermal decomposition, phase identification, morphology, ionic conductivity of the samples were studied by TGA/DTA, XRD and SEM four probe D.C. method respectively. The formation of $Nd_2Mo_2O_9$ was confirmed by FTIR studies. The synthesis and crystallization were followed by thermochemical techniques (TGA/DTA) studies. The synthesized materials showed reasonable ionic conductivity. These results indicate that assisted combustion method is a promising method to prepare nanocrystalline $Nd_2Mo_2O_9$ for solid oxide fuel cell.***

Keywords: Ionic Conductivity, Scanning Electron Microscopy, Transmission Electron Microscope, X-ray Diffraction, and FTIR.

I. INTRODUCTION

Solid oxide fuel cells (SOFCs) which convert chemical energy directly into electrical energy have been viewed as promising new power-generating systems and true multi-fuel energy devices. Recently significant efforts have been directed towards the development of intermediate temperature solid oxide fuel cell (IT-SOFC) due to its high power density and high working efficiency when operated around 500-800˚C. Mixed ionic-electronic conductivity (MIECs) have attracted the attention of researchers due to high thermal and chemical stability along with high oxygen diffusion and electronic conductivity.

The efficiency of energy conversion of an SOFC and its performance durability mainly depend on the oxide ion conducting solid electrolyte activity. The Neodymium molybdate forms a large family of materials with interesting physical properties. These properties depend on the crystal structures of these oxides, as well as on the oxidation state of molybdenum. In the case of the highest oxidation state of molybdenum +VI, the recent discovery of the fast oxide-ion conductor, $La_2Mo_2O_9$ has attracted considerable interest for its potential applications.

In the present work, synthesis of $Nd_2Mo_2O_9$nano powders using different molar ratios by assisted combustion method. The effect of different ratios on phase evaluation, size, and shape of the $Nd_2Mo_2O_9$particles were studied. Oxide materials with high mobility of oxygen ion receive extensive attention owing to the potential applications in solid oxide fuel cells, oxygen sensors, oxygen pumps, and oxygen-permeable membrane catalysts.

II.EXPERIMENTAL AND CHARACTERIZATION

The$Nd_2Mo_2O_9$powder was synthesized by assisted combustion method using high purity $Nd(NO_3)_2$(Sigma Aldrich, >99.9%), MoO_3(Sigma-Aldrich, >99.9%), and aspartic acid (Sigma Aldrich, >99.9%), as fuel. All of the reagents, in requisite stoichiometry amounts of the starting materials, were dissolved in the double distilled deionized water in order to obtain a homogeneous solution. A gel was appeared after continuous stirring at 80˚C for depending on the element. The foamy powder was crushed in a pestle and mortar. The crushed powder was kept in a muffle furnace at 600°C for hours 6 to get a single- phase nanocrystalline powders.

III. STRUCTURAL CHARACTERIZATION ANALYSIS

The structural properties of the synthesized material using X-ray diffraction studies (Model: Philips X' pert MPD). The diffraction patterns were recorder using Cu-Kα radiation at room temperature in the range of $10^\circ \leq 2\theta \leq 70^\circ$. The X-ray data were recorded in terms of the diffracted X-ray intensities (I) vs 2θ. The crystalline size was calculated with the help of scherrer's formula, which is given as

$$D = 0.9\lambda/\beta\cos\theta,$$

Where D is the crystallite size, β is the full-width at half-maximum (FWHM) of the most intensity \W diffraction peak in radians, θ is the diffraction angle and λ is the wave length of X-ray radiation. The particle size and morphology of the produced powder were analysed with a JEOL scanning electron microscopy SEM (Model: JSM-840A) equipment.

The thermal decomposition of the polymeric precursors was characterized by perkin-Elmer TG/DTA thermal analysis (Model; Pyris Diamond). The TGA is a process which relies on measuring the change in physical and chemical properties of a sample as a function of temperature or as a function of time.

IV.Result and Discussion

a. *Analysis of Crystal Structure*

Typical X-ray powder diffraction (XRD) patterns of $Nd_2Mo_2O_9$is shown in Fig 4.1. In general, all the diffracted peaks are broader than usually observed for highly crystalline powder. The lattice parameter calculated for the synthesized$Nd_2Mo_2O_9$, the broadening of the diffracted peaks is attributed to the superfine crystalline nature of composites. These results are in good agreement with the result of the orthorhombic structure. The size of the particles was calculated by Scherrer equation it was 30 nm. All diffraction peaks of the samples can be indicated to the orthorhombic structure without the formation of other impurities. The particles of the synthesized products are in nano range.

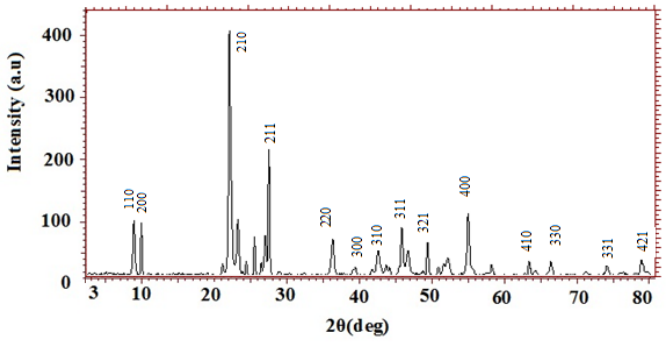

Fig. 1.X-ray diffraction pattern of $Nd_2Mo_2O_9$

b. Scanning Electron Microscopy

Fig.4.2 shows the SEM microstructure of $Nd_2Mo_2O_9$ powder obtained at 550°C for 6 hours. The surface morphology of the synthesized product was different pores and grains. Further, the SEM image indicates that the particles are agglomeration. The average crystallite size was 30 nm. The particles are uniformly distributed. There is an agglomerate of the particles. The particles of the synthesized products are in nano range

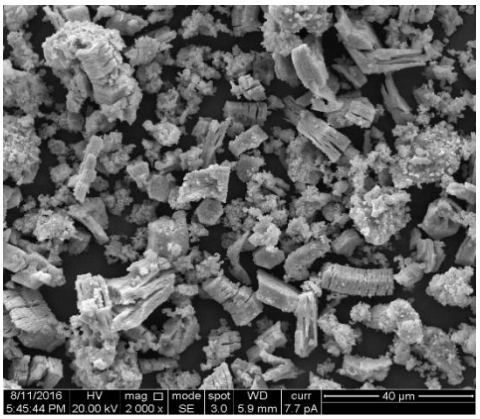

Fig.2.SEM photograph of Nd2Mo2O9

c. Thermal Analysis

TGA/DTA

Fig 4.3.shows that TGA/DTA pattern obtained on $Nd_2Mo_2O_9$ powder. In the TGA pattern, the $Nd_2Mo_2O_9$ sample showed a weight loss of about 0.052 mg/min until 100˚C. The sample on further heating from 100˚C-800˚C showed slight weight gain and loss of about 0.052mg/min. Again the sample showed a weight increase from 109.43˚C-386.39˚C of 0.688mg/min. The weight gain and weight loss indicated that the $Nd_2Mo_2O_9$ powder exhibited easily reversible absorption-desorption of oxygen from the air. The chemical decomposition with increases of temperature was examined through DTA and it appeared as the endothermic and exothermic peaks in the DTA curve. From the DTA curve, it is seen that a broad exothermic peak at 586.830˚C occurred due to

weight lose between 39.92˚C-723.50˚C in TGA curve. From the above TGA/DTA data, we know the $Nd_2Mo_2O_9$gradually absorbs the oxygen from air with temperature.

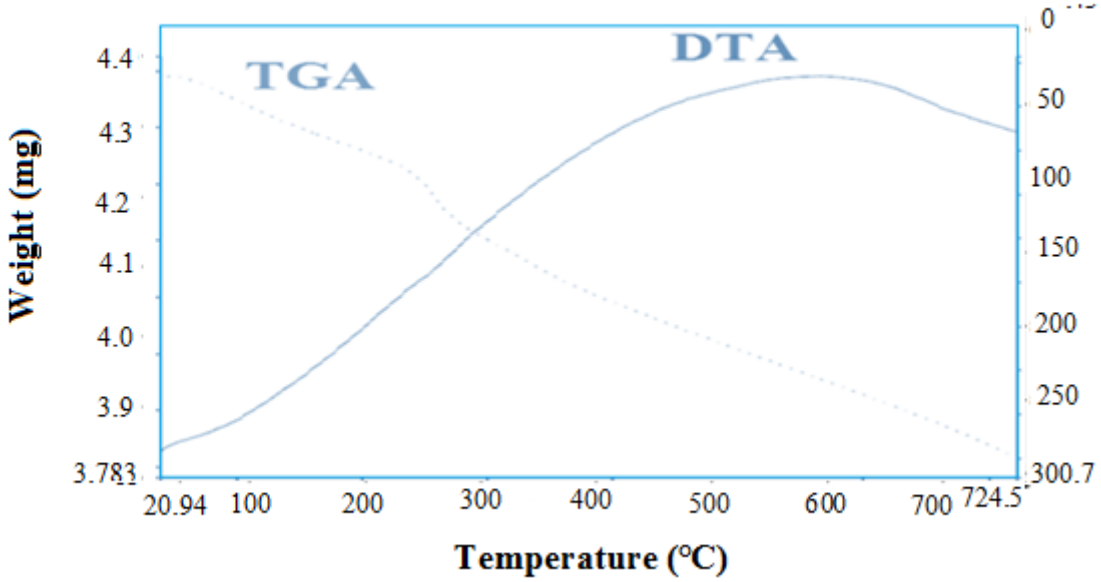

Fig. 3.TGA and DTA of Nd2Mo2O9

d. FTIR Analysis

FTIR spectroscopy was used to verify the functional groups present in the crystalline substance which range of 4000 cm^{-1} to400cm^{-1} as shown in fig.4.4. The broadband at 3600.9cm^{-1} can be assigned to vibration mode of chemically bonded hydroxyl groups. The powder exhibited a strong bond at 600-1000 cm^{-1} due to the stretching mode of Mo-O bond in the structure. The peak appeared at 816.1 cm^{-1} corresponds to the H-O-H bond mode confirming the presence of moisture in the sample. The peak appeared at 1354.6 cm $^{-1}$ is due to the presence of CO_2 in the sample. The sample$Nd_2Mo_2O_9$ exhibited a low-intensity peak at 816.1 cm $^{-1}$ sample exhibited two peaks obtained between the wavelength regions 800-1400 cm^{-1} and observed at 816.1, 1354.6, and 3600.9 cm $^{-1}$. The peak appeared at 1354.6 cm^{-1} is related to the O-H stretching vibration of H_2O in the sample. The broadband at 3600.9cm^{-1} can be assigned to vibration mode of chemically bonded hydroxyl groups.

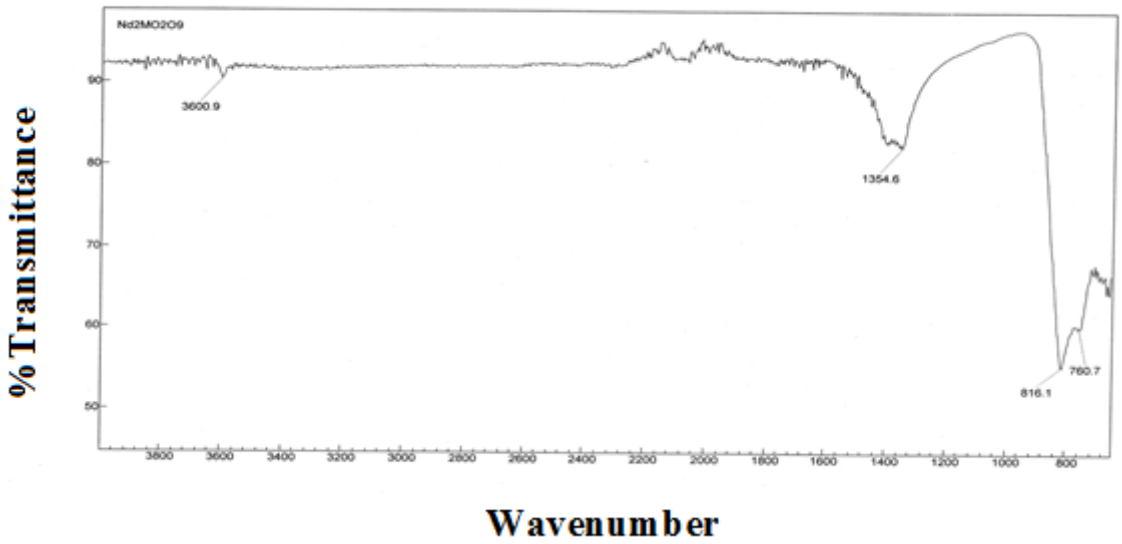

Fig 4.FT-IR spectrum of Nd2Mo2O9

e. Ionic Conductivity and its Temperature Dependence

The ionic conductivity of $Nd_2Mo_2O_9$ at 800˚C is used for SOFC electrolyte application. The Arrhenius plot for the overall conductivity of $Nd_2Mo_2O_9$ pellet sintered at 800˚C for 6 h is shown in 4.5. It shows clearly a first-order transition at 560˚C with the increasing conductivity. At 750˚C it exhibits a conductivity of 0.160S/cm. The estimated ionic transport number is slightly decreased with increasing temperature. This result demonstrates that the conductivity of $Nd_2Mo_2O_9$ is mainly ionic in nature.

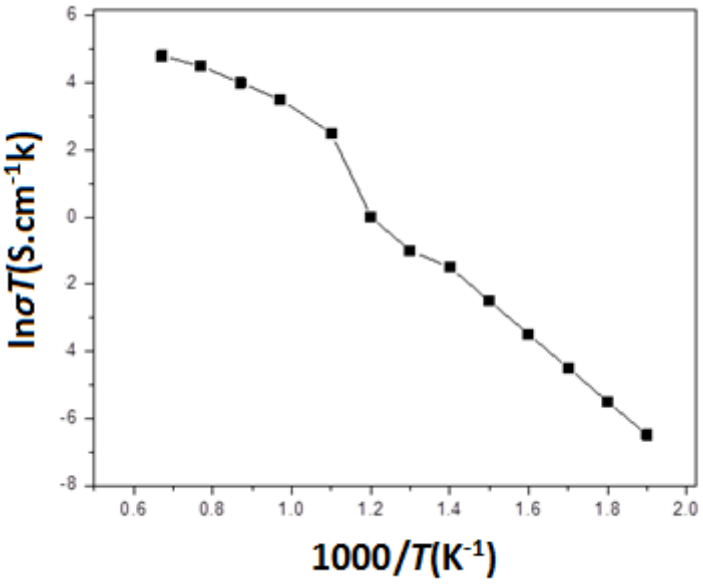

Fig. 5. Arrhenius plot of the overall conductivity of Nd2Mo2O9 pellet sintered at 800˚C for 6 h

CONCLUSION

The present investigation was carried out to improve the performance of $Nd_2Mo_2O_9$ by the synthesis method. The electrochemical behavior of $Nd_2Mo_2O_9$ based materials depends upon the method of synthesis and sintering temperature nanocrystalline materials. The present work was mainly focused on synthesis and ionic conductivity of $Nd_2Mo_2O_9$.

REFERENCE

[1] [G. Corb.el, # Y. Laligant, # F. Goutenoire, # E. Suard,# and P. Lacorre*,#, *Effects of Partial Substitution of Mo^{6+} by Cr^{6+} and W^{6+} on the Crystal Structure of the Fast Oxide-ion Conductor Structural Effects of W^{6+}*, 17,4678-4684.] Chem. Mtter.2005,`

[2] [Stuart A Hayward and Simon A T Redfern, *Thermodynamic nature of and spontaneous strain below the cubic-monoclinic phase transition in $La_2Mo_2O_9$*, J.phys: condense. Matter 16 (2004) .3571-3583.]

[3] A.P. Khandale[a], R.P. Lajurkar[a,b], S.S.Bhoga[a,*], *$Nd_{1.8}Sr_{0.2}Ni_{4-\delta}$: $Ce_{0.9}Gd_{0.9}O_{2-\delta}$ composite cathode for intermediate temperature solid oxide fuel cells, International journal of Hydrogen energy 39* (2014) 19039-19050.

[4]1.A.P.Khandale, S.S.Bhonga* *Combistion synthesized $Nd_{2-x}Ce_xCu0_4$ (X= 0-0.25) cathode δmaterials for intermediate temperature solid oxide fuel cell applications, Journal of power sources 195* (2010) 7974-7982.

[5] G. Caboura[a, *], G. Caboche[a], S.Chevalier[a] , P. Piccardo[b], *Opportunity of metallic interconnects for ITSOFC: Reactivity and electrical property, Journal of power sources 156* (2006) 39-44.

[6] J. G. de M. Furtado [1], C. A. da Silva [2], P. E. V. de Miranda [3]*Microstructure Densification and Electrical Performance of yttria stabilized zirconia sofc electrolyte, 19˚ congress brasileiroengenhariaciencia dos materials-CBECiMat, 21 a 25 de novembro de* 2010, Campos do Jordao, SP, Brasil.

[7]Baijun Yan, Jiahua Liu, Yunduo Dai, Qifeng Shu, and Zhihua Ren, *Molar heat capacities of $La_2Mo_2O_9$ and $La_{1.9}Sr_{0.1}Mo_2O_{9-\delta}$* , Journal of University of science and technology Beijing Volume 14, Number 5, October 2007, page 395.

[8] Q.F.Fang* , X.P.Wang, Z.S.Li , G.G. Zhang , Z.G. Yi , *Relaxation peaks associated with the oxygen- ion diffusion in $La_{2-1}Bi_xMo_2O_9$ oxide-ion conductors* , Material Science and Engineering A 370 (2004) 365-369.

